Published February 25, 2013

The voltage-sensing domain of a phosphatase gates the pore of a potassium channel

Cristina Arrigoni,[1] Indra Schroeder,[3] Giulia Romani,[2] James L. Van Etten,[4,5] Gerhard Thiel,[3] and Anna Moroni[1,2]

[1]Department of Biosciences and [2]Institute of Biophysics, Consiglio Nazionale delle Ricerche, Università degli Studi di Milano, 20133 Milano, Italy

[3]Plant Membrane Biophysics, Technische Universität Darmstadt, 64287 Darmstadt, Germany

[4]Department of Plant Pathology and [5]Nebraska Center for Virology, University of Nebraska, Lincoln, NE 68583

The modular architecture of voltage-gated K^+ (Kv) channels suggests that they resulted from the fusion of a voltage-sensing domain (VSD) to a pore module. Here, we show that the VSD of *Ciona intestinalis* phosphatase (Ci-VSP) fused to the viral channel Kcv creates Kv_{Synth1}, a functional voltage-gated, outwardly rectifying K^+ channel. Kv_{Synth1} displays the summed features of its individual components: pore properties of Kcv (selectivity and filter gating) and voltage dependence of Ci-VSP ($V_{1/2}$ = +56 mV; z of ~1), including the depolarization-induced mode shift. The degree of outward rectification of the channel is critically dependent on the length of the linker more than on its amino acid composition. This highlights a mechanistic role of the linker in transmitting the movement of the sensor to the pore and shows that electromechanical coupling can occur without coevolution of the two domains.

INTRODUCTION

K^+ channels are modular proteins, composed of a central pore module (PM) surrounded by sensor domains that perceive external stimuli and convert them into changes of pore activity (gating). This feature and simple assessment of their performance by electrophysiological measurements make ion channels amenable for testing the hypothesis that the pore of voltage-gated K^+ (Kv) channels acquired the voltage-sensing domain (VSD) throughout evolution. The modular building concept has several implications. First, it suggests that single domains, once detached from the original channel, can function independently; for instance, the PM of the bacterial KvLm channel forms a functional K^+ channel when separated from its VSD domain (Santos et al., 2008). Second, regulatory modules, which control K^+ channels, are also found in proteins with completely different enzymatic functions. A VSD displaying the hallmarks of those of Kv channels is connected to a soluble phosphatase in the sea squirt *Ciona intestinalis* phosphatase (Ci-VSP) protein (Murata et al., 2005). Third, modularity also implies that domains of different classes of channels can be swapped. So far, attempts to exchange entire membrane modules between K^+ channels have been unsuccessful, leaving this third implication unfulfilled (Caprini et al., 2001). Only small portions of the two domains, the "paddle" motif of the VSD and the P loop with most of the transmembrane domains of the pore, could be exchanged between K^+ and Na^+ channels (Lu et al., 2001; Alabi et al., 2007; Bosmans et al., 2008; Ben-Abu et al., 2009). From this it was concluded that membrane modules have coevolved so intimately in Kv proteins that it is impossible to exchange them entirely without losing functionality of the chimeric channels.

Here, we show that it is possible to obtain a voltage-gated channel in one step by fusing two full-length modules: the VSD of Ci-VSP and the PM of the viral K^+ channel Kcv (Plugge et al., 2000). These two membrane modules are evolutionarily unrelated, and there is not any "a priori" indication that they should be able to make a voltage-sensitive channel. The *Ciona* VSD regulates a soluble enzyme, yet it remains speculative if this sensor would gate a channel pore. The second component, the viral channel Kcv, is clearly not designed to be controlled by external stimuli, such as voltage. Apart from a 12–amino acid-long N terminus, the channel comprises only the bare PM and has neither additional membrane nor cytosolic domains (Plugge et al., 2000).

Correspondence to Anna Moroni: anna.moroni@unimi.it

Abbreviations used in this paper: Ci-VSP, *Ciona intestinalis* phosphatase; Kv, voltage-gated K^+; PM, pore module; TEVC, two-electrode voltage clamp; VSD, voltage-sensing domain.

The Rockefeller University Press $30.00
J. Gen. Physiol. Vol. 141 No. 3 389–395
www.jgp.org/cgi/doi/10.1085/jgp.201210940

Published February 25, 2013

MATERIALS AND METHODS

Chimeric constructs

All constructs were inserted into BamHI and XhoI restriction sites of pSGEM vector (a modified version of pGEM-HE). In vitro transcription was performed on linearized plasmids using T7 RNA polymerase (Promega), and cRNAs were injected (50 ng per oocyte) into *Xenopus laevis* oocytes, as reported previously (Plugge et al., 2000). Electrophysiological measurements were made 3–4 d after injection. Mutations were inserted by site-directed mutagenesis (QuikChange site-directed mutagenesis kit; Agilent Technologies) and confirmed by sequencing. Chimeric constructs were generated by overlapping PCR from Ci-VSP (provided by D. Minor, University of California, San Francisco, San Francisco, CA) and PBCV-1 Kcv. Kv_{Synth1} includes amino acids 1–239 of Ci-VSP and amino acids 1–94 of Kcv. All constructs reported in Fig. 3 were obtained with this procedure.

Electrophysiological measurements

Two-electrode voltage-clamp (TEVC) experiments were performed as indicated previously (Plugge et al., 2000) using an amplifier (GeneClamp 500; Axon Instruments) and filtered at 5 kHz. Data acquisition and analysis were done using the pCLAMP8 software package (Axon Instruments). Electrodes were filled with 3 M KCl and had a resistance of 0.2–0.8 MΩ in 50 mM KCl. The oocytes were perfused at room temperature (25–27°C) at a rate of 2 ml/min with a bath solution containing 50 mM KCl (or NaCl), 1.8 mM $CaCl_2$, 1 mM $MgCl_2$, and 5 mM HEPES, adjusted to pH 7.4 with KOH (or NaOH). Mannitol was used to adjust the osmolarity of the solution to 215 mosmol/l. $BaCl_2$ diluted from 1-M stocks was added to the solution as indicated. The standard clamp protocol consisted of steps from the holding voltage of −20 mV to voltages in the range of −100 to +100 mV; tail currents were measured at −80 mV. Instantaneous and steady-state currents were sampled after 10 ms and at the end of the voltage step, respectively.

For single-channel recordings, the vitelline membrane of the oocytes was removed mechanically before the experiment. Patch pipettes were made from borosilicate glass and had a resistance of 2–5 MOhm. Bath and pipette solution for measurements with Kcv_{PBCV1} contained 100 mM KCl, 1.8 mM $CaCl_2$, 1 mM $MgCl_2$, and 10 mH HEPES, adjusted to pH 7.4 with KOH. Experiments with Kv_{Synth} were done with 150 mM KCl. The slightly different K^+ concentrations (150 mM for KvSynth and 100 mM for WT) do not impede comparison. According to Pagliuca et al. (2007), the difference in conductance for the WT would be 20% at most, which is well within the error bars. Currents were recorded with an amplifier (DAGAN3900; Dagan Corporation) and a digitizer unit (LIH8+8; HEKA).

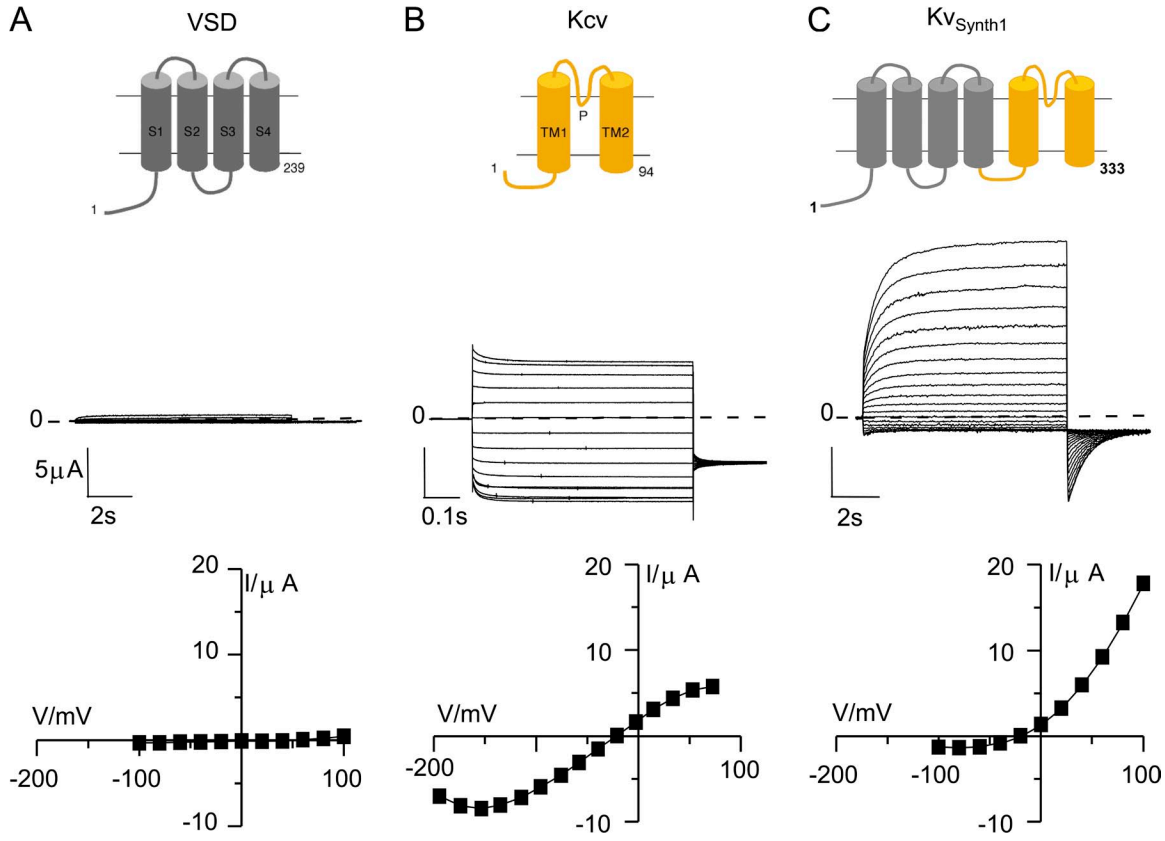

Figure 1. The synthetic channel Kv_{Synth1} is an outward rectifier. (Top) Cartoons of the individual components and of the fusion protein Kv_{Synth1}. (A) VSD is the voltage-sensing domain (amino acids 1–239) of Ci-VSP; S1–S4 indicate the four transmembrane domains of the VSD. (B) Kcv is the full-length (amino acids 1–94) viral K^+ channel; TM1, TM2, and P indicate, respectively, the two transmembrane domains and the pore loop of Kcv. (C) Kv_{Synth1} is the 333–amino acid fusion protein of VSD and Kcv. (Middle) Currents recorded by TEVC in oocytes injected with the respective constructs. Dotted line indicates zero current level. Voltage protocol: V_h, −20 mV; test voltages, +100 to −100 mV (−200 mV for Kcv); tail, −80 mV. Test pulse length: A and C, 8.5 s; B, 0.6 s. (Bottom) Corresponding steady-state I-V relationships. All experiments were performed in 50 mM $[K^+]_{out}$.

Published February 25, 2013

RESULTS

To test whether the voltage-dependent movement of the *Ciona* VSD is able to gate a channel, we created the fusion protein Kv_{Synth1} by adding amino acids 1–239 of Ci-VSP to the full-length Kcv sequence (amino acids 1–94). The fusion protein and its individual components have been expressed in *Xenopus* oocytes and tested by TEVC. Control experiments show that VSD-injected oocytes (Fig. 1 A) generate small currents, not different from typical water-injected oocytes. Oocytes expressing Kcv alone (Fig. 1 B) show the typical K^+ currents, which have been characterized previously (Moroni et al., 2002; Gazzarrini et al., 2004, 2006; Kang et al., 2004; Abenavoli et al., 2009). The I-V relationship of Kcv is linear at moderate voltages. At extreme voltages, the ohmic behavior is lost because of a fast gating mechanism that occurs at the selectivity filter and results in a negative slope conductance (Abenavoli et al., 2009). Kv_{Synth1} generates currents that are very different from those of its single components and shows the typical properties of a delayed-rectifier K^+ channel, slowly activating at positive potentials (Hille, 1992) (Fig. 1 C). Depolarizing voltages generate large time-dependent currents on top of a small instantaneous component. The corresponding steady-state I-V relationship shows a strong outward rectification. To quantify the degree of rectification, we use the ratio of steady-state currents at +60/−100 mV (I_{+60mV}/I_{-100mV}). For Kv_{Synth1}, it is 13.3 ± 2 (average of six oocytes); this ratio is 1 ± 0.1 in Kcv.

Kv_{Synth1} has the permeability properties of Kcv. Replacement of external K^+ with Na^+ shifts the reversal voltage of the fully activated Kv_{Synth1} current by −80 mV ± 6 (SD, n = 3 oocytes) (Fig. 2 A) and reduces the outward current, another typical feature of Kcv (Plugge et al., 2000). The estimated relative permeability P_{Na}/P_K of 0.05 ± 0.01 closely resembles the value of 0.03 ± 0.01 reported previously for Kcv (Chatelain et al., 2009).

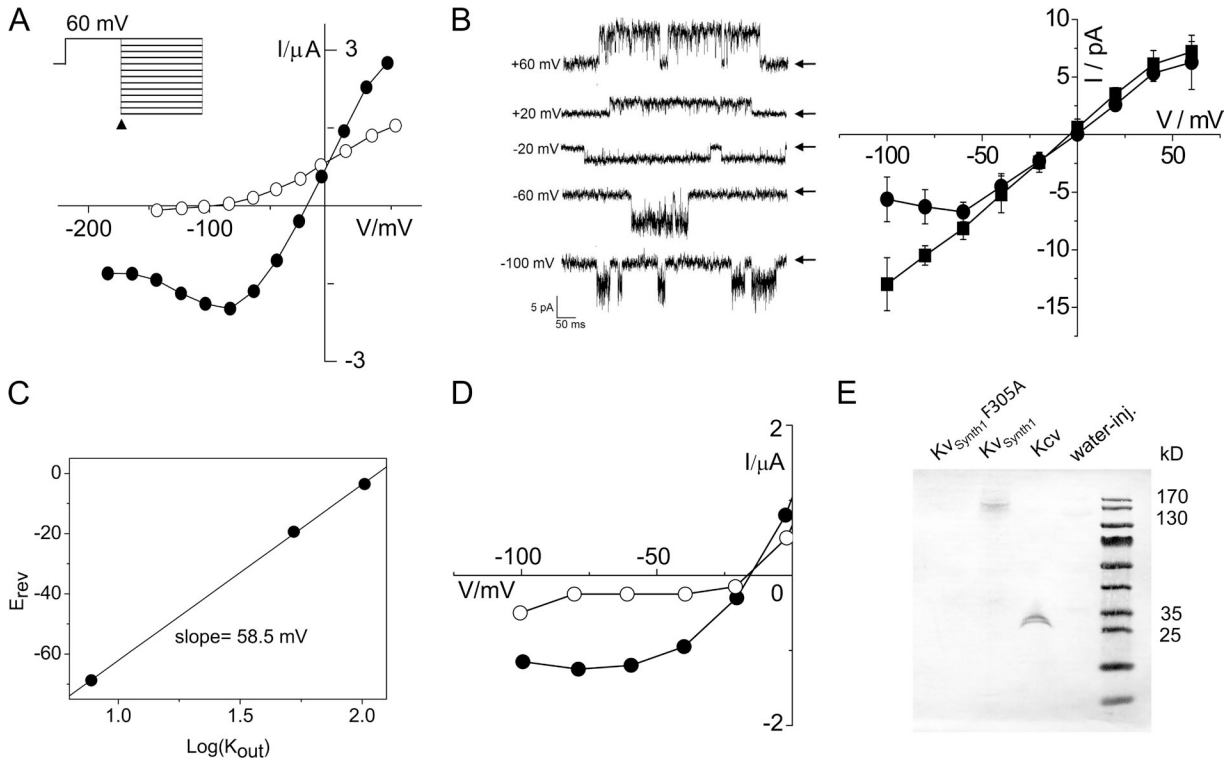

Figure 2. Biophysical and biochemical properties of Kv_{Synth1}. (A) Kv_{Synth1} selects K^+ over Na^+. Current reversal potential recorded from the same oocyte was −20 mV in 50 mM $[K^+]_{out}$ (●) and −98 mV in 50 mM $[Na^+]_{out}$ (○). Voltage protocol: prepulse voltage step at +60 mV, followed by testing voltages from +60 to −180 mV. Arrowhead marks the point of data collection. (B) Single-channel properties of Kv_{Synth1}. (Left) Representative opening burst at different membrane voltages, with arrows denoting the baseline. The open probability in the presented sections is not representative. The low-pass filter was set to 20 kHz, the sampling rate was 100 kHz, and traces were digitally filtered at 2 kHz for clarity. (Right) Comparison of the I-V curves of Kv_{Synth1} in 150 mM K^+ (●) and Kcv in 100 mM K^+ (■). Symbols represent mean and standard deviation of three experiments. (C) Nernst plot: current reversal potential (E_{rev}) of macroscopic Kv_{Synth1} current plotted as a function of external K^+ concentration (Lg[K^+]out). Black line is the linear regression to E_{rev} mean values (n = 3). (D) Effect of barium on Kv_{Synth1} current. Steady-state currents recorded in (●) control solution (50 mM K^+) and (○) plus 1 mM $BaCl_2$. Currents recorded from a holding potential (V_h) of −20 mV to the indicated test voltages. Test pulse length was 8.5 s. The addition of barium blocks the inward current and moderately affects the outward current, as reported previously for Kcv channel (Plugge et al., 2000). (E) Western blot analysis performed on total protein extracts with a custom-made antibody (8D6) recognizing the tetramer, but not the monomer, of Kcv. The expected molecular mass of Kcv and Kv_{Synth1} tetramers are 42.5 and 149 kD, respectively.

Published February 25, 2013

Another feature of Kcv that is preserved in Kv_{Synth1} is the aforementioned negative slope conductance of the open channel, in this case already visible at approximately −100 mV (Fig. 2 A). This feature is confirmed by the single-channel measurements reported in Fig. 2 B showing clear flickering behavior with a consequent reduction of the unitary channel conductance at voltages negative of approximately −100 mV.

The single-channel I-V relationship (I-V curve) of Kv_{Synth1} reported in Fig. 2 B together with that of Kcv for comparison shows that at membrane voltages more negative than −60 mV, the current of Kv_{Synth1} decreases, resulting in a negative slope conductance. The Kcv channel shows this behavior only at more negative voltages, beyond −100 mV (Abenavoli et al., 2009). This is consistent with the observation that the instantaneous currents of Kv_{Synth1} in TEVC experiments (Fig. 2 A) begin the negative slope conductance earlier than the WT Kcv. The conductance of the synthetic channel (112 ± 25 pS between −50 and +50 mV) is only slightly smaller than that of Kcv (133 ± 8 pS, also reported previously by Abenavoli et al., 2009, as 114 ± 11 pS). This confirms that the general filter structure and function are not dramatically altered by the addition of the voltage sensor. Fig. 2 summarizes other Kcv properties preserved in Kv_{Synth1}, including K^+ selectivity shown by the slope of 58.5 mV in the Nernstian plot of Fig. 2 C, voltage-dependent barium block of the instantaneous inward current shown in Fig. 2 D, and the evidence that the synthetic protein forms a stable tetramer. Fig. 2 E shows a Western blot decorated with an antibody raised against the Kcv tetramer that does not recognize the monomer. The same antibody recognized Kv_{Synth1} WT at about the predicted molecular mass of the tetramer

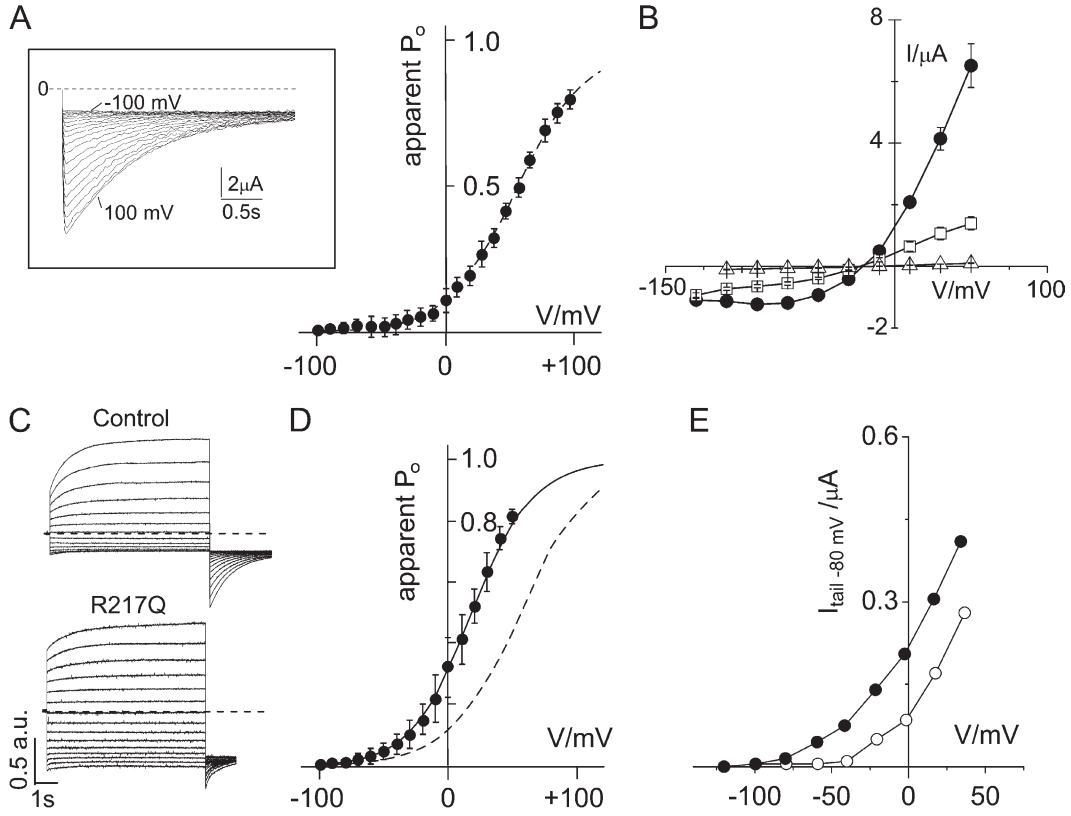

Figure 3. Voltage dependency of Kv_{Synth1}. (A) Activation curve of Kv_{Synth1} constructed from tail currents (inset) after subtracting the instantaneous current offset. Voltage protocol as in Fig. 1 C. Datasets ($n = 6$) were jointly fitted to a two-state Boltzmann equation (dotted line) of the form $y = (1 + e^{zF(V - V_{1/2})/RT})^{-1}$, where z is the effective charge; $V_{1/2}$ is the half-activation voltage; and F, R, and T have their usual thermodynamic meaning. Data were normalized to the extrapolated maximum current. Points represent mean ± SEM. $V_{1/2} = 56$ mV and $z = 0.92$. (B) Steady-state I-V relationships of the single mutant F305A (△), the double mutant R229Q/R232Q (□), and the WT Kv_{Synth1} (●). Points represent mean ± SEM ($n = 6$). Currents were recorded from a holding potential (V_h) of −20 mV to the indicated test voltages (pulse length, 600 ms). (C) Exemplary currents recorded from WT Kv_{Synth1} (control) and its R217Q mutant. To compare currents from different constructs, the traces have been normalized to the current value recorded at +60 mV and expressed in arbitrary units (a.u.). Voltage protocol as in Fig. 1 C. (D) Activation curve of the R217Q mutant (●) constructed as in A from four datasets: $V_{1/2} = 18$ mV and $z = 1.1$. The curve of the WT (dotted line) is replotted from A for comparison. (E) The activation of the R217Q mutant depends on the preconditioning voltage. The same R217Q-expressing oocyte was subjected to the following protocol: preconditioning (5 s) at either −100 or +40 mV and test pulses from −120 to +30 mV. Tail currents (at −80 mV) are plotted for preconditioning at −100 mV (○) or at +40 mV (●). The test pulses were kept short (1.2 s) to maintain the effect of the preconditioning voltages; hence, data in E do not reflect full activation of the channel.

Published February 25, 2013

(149 kD). Interestingly, mutation F305A in the K^+ channel signature sequence (GFG) of Kv_{Synth1} prevented antibody recognition, indicating that either the protein is not synthesized or, more likely, does not form a stable tetramer. Accordingly, this mutant produced no measurable current when tested in TEVC (Fig. 3 B). In summary, Kv_{Synth1} displays the pore properties of Kcv, such as selectivity, fast gating, and overall pore architecture; these are not modified by the addition of the VSD.

The new property introduced by the VSD is a strong voltage dependency of the currents. The voltage sensor closes the channel at negative potentials and opens it with a slow kinetics at voltages more positive than 0 mV ($t_{1/2}$ = 450 ± 74 ms at +60 mV; n = 4 oocytes) (Fig. 1 C). The activation curve shown in Fig. 3 A was determined from the tail currents after subtraction of the instantaneous component (inset of Fig. 3 A). Even though full saturation of the open probability could not be reached for the presence of endogenous conductances in oocytes, the activation curve could be fitted with a Boltzmann equation. Kv_{Synth1} has an apparent half-activation voltage ($V_{1/2}$) of +56 mV, and channel opening is caused by the movement of the equivalent of about one electronic charge across the membrane (z = 0.92). These parameters strongly resemble those reported for the sensing currents of Ci-VSP, either with or without the phosphatase (Murata et al., 2005; Villalba-Galea et al., 2008). To confirm that the VSD is responsible for the voltage-dependent properties of Kv_{Synth1}, we replaced two of the four arginines in the S4 segment, R229 and R232, with glutamines. In Ci-VSP, this double mutation eliminates the "sensing" currents and generates a voltage-insensitive phosphatase (Murata et al., 2005; Murata and Okamura, 2007). In Kv_{Synth1}, the double mutation R229Q/R232Q results in a very small and quasi-ohmic current (3B); the mutated VSD has apparently lost its tight control on channel opening and voltage dependency. Another interesting mutation that shifts the Q-V curve of Ci-VSP to the left by 46 mV is the single neutralization of the gating charge R217 to Q

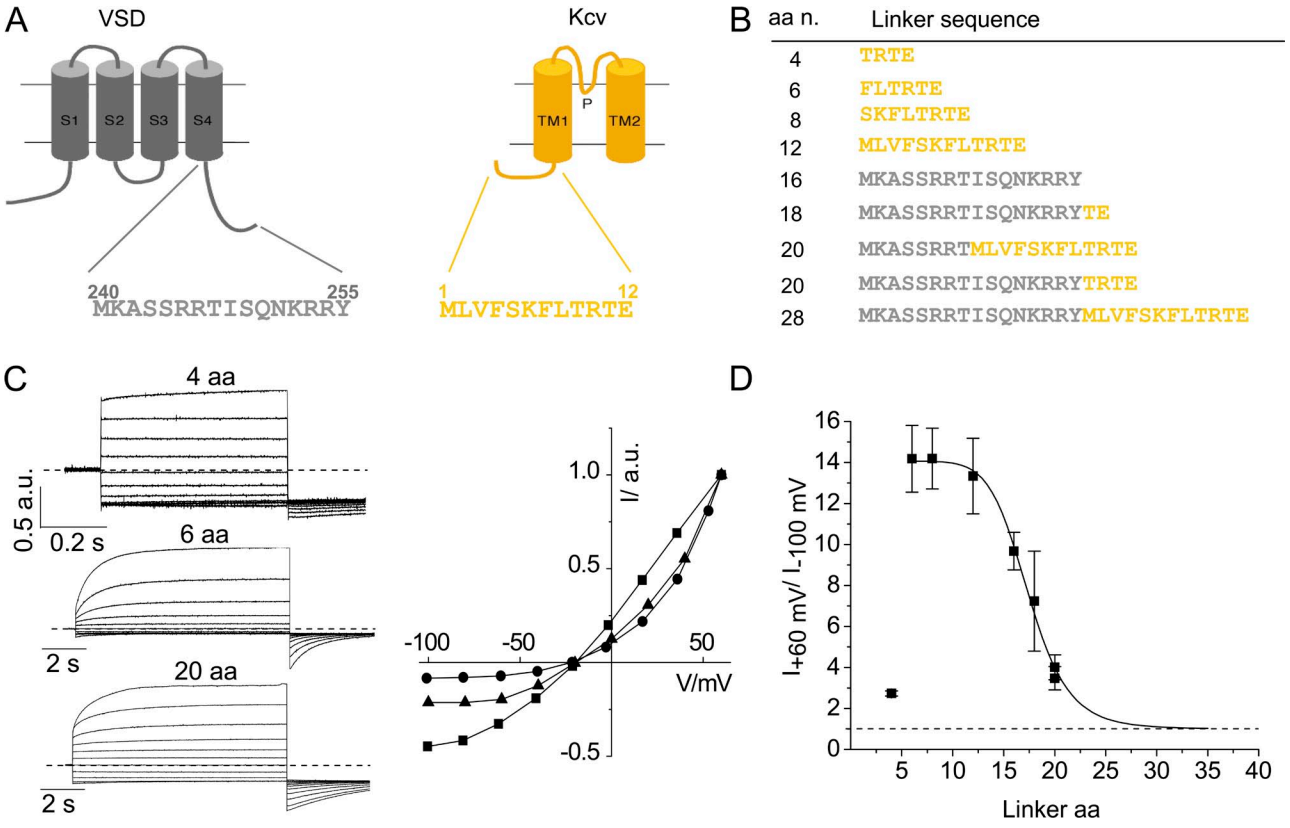

Figure 4. The length of the linker connecting the VSD to the pore affects the degree of rectification in Kv_{Synth1} constructs. (A) Expanded view of the sequences of the two sequences that where variably combined to form the Kv_{Synth1} linker. (B) List of linkers that have been tested in Kv_{Synth1}, their amino acid (aa) length, and amino acid sequences (color coded as in A). (C) Exemplary current traces recorded from Kv_{Synth1} constructs with the 4–, 6–, and 20–amino acid linkers and their corresponding I-V relationships (color coded). To compare currents from different constructs, the traces have been normalized to the current value recorded at +60 mV and expressed in arbitrary units (a.u.). Voltage protocol as in Fig. 1 C. (D) The degree of current rectification (I_{+60mV}/I_{-100mV}) is plotted as a function of linker length for all functional constructs. Data are mean ± SEM ($n \geq 3$). Experimental data (with the exclusion of the value corresponding to the construct with a 4–amino acid linker that loses the rectification) have been interpolated with a logistic function (black line) in which the lower asymptote was set to 1, corresponding to the value measured in Kcv that lacks rectification (dotted line).

Published February 25, 2013

(Villalba-Galea et al., 2008). The same mutation in Kv_{Synth1} resulted in a channel that is already more open at the holding voltage because the activation curve is shifted by 38 mV to the left (Fig. 3, C and D). Judging from the behavior of these mutants, we conclude that the properties of the VSD are transmitted to the gating of the pore. To examine further details of the causal interplay between VSD and channel gating, we tested whether Kv_{Synth1} also reveals the mode shift, which has been described for the sensor domain (Villalba-Galea et al., 2008). During a long-lasting depolarization, the voltage sensor enters a "relaxed" conformation in which the voltage dependency is markedly shifted toward negative potentials. To test this, we measured the tail currents of Kv_{Synth1} R217Q after holding the same oocyte at two different preconditioning voltages, −100 and +40 mV for 5 s. Tail currents were collected at −80 mV after prepulse at different voltages that were kept short (1.2 s) to limit the effect on the relaxation. Fig. 3 E shows that the resulting I_{tail}/V curve is shifted to more negative potentials when the oocyte is preconditioned at +40 mV. The observed negative shift of ∼30 mV ($n = 3$ oocytes) matches quite well the direction and the amplitude of the shift reported for the VSD (Villalba-Galea et al., 2008). These data further confirm that the properties of the sensor are transmitted to the gating of the pore.

Considerable evidence supports the role of the S4–S5 linker in Kv channels as the transducing element between sensor movement and pore gating (Long et al., 2005). In Kv_{Synth1}, the VSD is directly connected to Kcv after removal of the 16–amino acid linker that in Ci-VSP couples the VSD to the phosphatase (Fig. 4, A and B). Hence, the 12–amino acid-long N terminus of Kcv acts here as the S4–S5 linker of Kv channels and transmits the conformational changes of the sensor to the pore. To study if and how the linker influences gating, we varied its length and composition by combining the N terminus of Kcv and the linker of the VSD, as shown in Fig. 4 B. All constructs produced functional channels, apart from that with the 28–amino acid linker that barely expressed and was not further analyzed. Fig. 4 C shows exemplary currents from constructs with 4–, 6–, and 20–amino acid linkers and their corresponding I-V relationships. The first and most cogent observation is that there is a minimum linker length required for efficient control of the voltage sensor on the pore, and that the transition is quite sharp. The construct with 4 amino acids is quite similar to the original channel Kcv, whereas that with 6 amino acids shows the typical features of Kv_{Synth1}, rectification and slow kinetics. Extending the linker up to 12 amino acids doesn't change significantly the properties of Kv_{Synth1} (not depicted), whereas trespassing this length results in a gradual disappearance of the properties, as shown by the construct with a 20–amino acid linker, with a predominant instantaneous component and an increase in inward current (see also the corresponding I-V curves in Fig. 4 C). This trend is summarized in Fig. 4 D, where we have plotted the degree of rectification (I_{+60mV}/I_{-100mV}) as a function of linker length, for all measurable constructs. Interestingly, rectification was not appreciably influenced by the amino acid composition because two constructs with a linker of the same length, 20 amino acids, but of different sequence (see Fig. 4 B), gave the same result.

DISCUSSION

The present data show that the coupling of Ci-VSD to Kcv is necessary and sufficient to transform a voltage-independent K^+ channel into a Kv-type outward rectifier. This finding has several corollaries. First, it shows unambiguously that the shallow voltage dependency of the S4 of *Ciona* VSD is sufficient to gate a channel pore. The activation curves of Kv_{Synth1} closely reflect the charge movement obtained with the isolated VSD in its WT and mutant form. Hence, the voltage-dependent features of the sensor are fully transmitted to the gating of the channel pore. Kv_{Synth1} exhibits the features of an outward rectifier, which conducts best at depolarizing voltages. This gain of function over the ohmic Kcv conductance can be explained with a model according to which the coupling with VS closes the pore of Kcv; the movement of the VS then causes a slow and voltage-dependent opening at positive voltages. From the shallow voltage dependency of Kv_{Synth1}, it can be speculated that the movement of a single VSD is probably sufficient for opening of the channel. Because the typical pore gating features of Kcv are still maintained in Kv_{Synth1}, the movement of the VSD is most likely operating a cytosolic gate of the channel; the latter is operated by salt bridge interactions at the cytosolic entrance of Kcv (Tayefeh et al., 2009).

Previous data implied that the pore and the voltage-sensor domains of Kv channels presumably required a tight coevolution at their interacting surfaces to achieve voltage-dependent gating (Long et al., 2005; Lee et al., 2009). In contrast, the present data show that a naive electromechanical coupling between an unrelated VSD and a pore is already sufficient for a voltage-dependent gating of the channel pore. The distinct coevolution between the sensor and the pore in modern Kv channels is therefore more likely a means to a fine-tuning of channel gating and not a basic structural requirement.

Another remarkable finding is that the effective voltage control of the VSD over the pore is a function of the linker length. It is evident that the linker must be longer than 4 amino acids and performs best with a length between 6 and 12 amino acids. This is in the range of linker length in Kv channels (Long et al., 2005).

Efficient coupling can be achieved in Kv_{Synth1} with completely unrelated linker sequences, such as the N terminus of Kcv and the C terminus of *Ciona* VSD (see Fig. 3). Even though we cannot exclude that both

Published February 25, 2013

linkers generate a similar fold, the data suggest that the length of the linker is more important for coupling of the two domains than its particular sequence. In this respect, the data are in good agreement with the idea that a rigid connection, which is presumably better provided by a short linker, favors the mechanical coupling between voltage sensor and pore (Long et al., 2005; Lee et al., 2009).

Third and lastly, the data show that a primitive channel with poor control on gating can acquire sophisticated voltage regulation via a naive fusion with a regulatory element from another source. This finding makes it likely that the appearance of Kv channels indeed occurred as a result of a singular evolutionary step, as suggested previously (Chanda and Bezanilla, 2008).

We thank Dan Minor (UCSF) for helpful discussion.

This work was partially supported by PRIN 2008, SAL-49 Progetto di Cooperazione Scientifica e Tecnologica Regione Lombardia, Cariplo 2009-3519 (to A. Moroni), LOEWE initiative Soft Control (to G. Thiel), National Science Foundation-EPSCoR (grant EPS-1004094 to J.L. Van Etten), and the COBRE program of the National Center for Research Resources (grant P20-RR15635 to J.L. Van Etten).

Christopher Miller served as editor.

Submitted: 19 November 2012
Accepted: 17 January 2013

REFERENCES

Abenavoli, A., M.L. DiFrancesco, I. Schroeder, S. Epimashko, S. Gazzarrini, U.P. Hansen, G. Thiel, and A. Moroni. 2009. Fast and slow gating are inherent properties of the pore module of the K^+ channel Kcv. *J. Gen. Physiol.* 134:219–229. http://dx.doi.org/10.1085/jgp.200910266

Alabi, A.A., M.I. Bahamonde, H.J. Jung, J.I. Kim, and K.J. Swartz. 2007. Portability of paddle motif function and pharmacology in voltage sensors. *Nature.* 450:370–375. http://dx.doi.org/10.1038/nature06266

Ben-Abu, Y., Y. Zhou, N. Zilberberg, and O. Yifrach. 2009. Inverse coupling in leak and voltage-activated K+ channel gates underlies distinct roles in electrical signaling. *Nat. Struct. Mol. Biol.* 16:71–79. http://dx.doi.org/10.1038/nsmb.1525

Bosmans, F., M.F. Martin-Eauclaire, and K.J. Swartz. 2008. Deconstructing voltage sensor function and pharmacology in sodium channels. *Nature.* 456:202–208. http://dx.doi.org/10.1038/nature07473

Caprini, M., S. Ferroni, R. Planells-Cases, J. Rueda, C. Rapisarda, A. Ferrer-Montiel, and M. Montal. 2001. Structural compatibility between the putative voltage sensor of voltage-gated K+ channels and the prokaryotic KcsA channel. *J. Biol. Chem.* 276:21070–21076. http://dx.doi.org/10.1074/jbc.M100487200

Chanda, B., and F. Bezanilla. 2008. A common pathway for charge transport through voltage-sensing domains. *Neuron.* 57:345–351. http://dx.doi.org/10.1016/j.neuron.2008.01.015

Chatelain, F.C., S. Gazzarrini, Y. Fujiwara, C. Arrigoni, C. Domigan, G. Ferrara, C. Pantoja, G. Thiel, A. Moroni, and D.L. Minor Jr. 2009. Selection of inhibitor-resistant viral potassium channels identifies a selectivity filter site that affects barium and amantadine block. *PLoS ONE.* 4:e7496. http://dx.doi.org/10.1371/journal.pone.0007496

Gazzarrini, S., M. Kang, J.L. Van Etten, S. Tayefeh, S.M. Kast, D. DiFrancesco, G. Thiel, and A. Moroni. 2004. Long distance interactions within the potassium channel pore are revealed by molecular diversity of viral proteins. *J. Biol. Chem.* 279:28443–28449. http://dx.doi.org/10.1074/jbc.M401184200

Gazzarrini, S., A. Abenavoli, D. Gradmann, G. Thiel, and A. Moroni. 2006. Electrokinetics of miniature K+ channel: open-state V sensitivity and inhibition by K+ driving force. *J. Membr. Biol.* 214:9–17. http://dx.doi.org/10.1007/s00232-006-0024-3

Hille, B. 1992. Ionic Channels in Excitable Membranes. Second edition. Sinauer Associates, Inc., Sunderland, MA. 607 pp.

Kang, M., A. Moroni, S. Gazzarrini, D. DiFrancesco, G. Thiel, M. Severino, and J.L. Van Etten. 2004. Small potassium ion channel proteins encoded by chlorella viruses. *Proc. Natl. Acad. Sci. USA.* 101:5318–5324. http://dx.doi.org/10.1073/pnas.0307824100

Lee, S.Y., A. Banerjee, and R. MacKinnon. 2009. Two separate interfaces between the voltage sensor and pore are required for the function of voltage-dependent K(+) channels. *PLoS Biol.* 7:e47. http://dx.doi.org/10.1371/journal.pbio.1000047

Long, S.B., E.B. Campbell, and R. Mackinnon. 2005. Voltage sensor of Kv1.2: structural basis of electromechanical coupling. *Science.* 309:903–908. http://dx.doi.org/10.1126/science.1116270

Lu, Z., A.M. Klem, and Y. Ramu. 2001. Ion conduction pore is conserved among potassium channels. *Nature.* 413:809–813. http://dx.doi.org/10.1038/35101535

Moroni, A., C. Viscomi, V. Sangiorgio, C. Pagliuca, T. Meckel, F. Horvath, S. Gazzarrini, P. Valbuzzi, J.L. Van Etten, D. DiFrancesco, and G. Thiel. 2002. The short N-terminus is required for functional expression of the virus-encoded miniature K(+) channel Kcv. *FEBS Lett.* 530:65–69. http://dx.doi.org/10.1016/S0014-5793(02)03397-5

Murata, Y., and Y. Okamura. 2007. Depolarization activates the phosphoinositide phosphatase Ci-VSP, as detected in Xenopus oocytes coexpressing sensors of PIP2. *J. Physiol.* 583:875–889. http://dx.doi.org/10.1113/jphysiol.2007.134775

Murata, Y., H. Iwasaki, M. Sasaki, K. Inaba, and Y. Okamura. 2005. Phosphoinositide phosphatase activity coupled to an intrinsic voltage sensor. *Nature.* 435:1239–1243. http://dx.doi.org/10.1038/nature03650

Pagliuca, C., T.A. Goetze, R. Wagner, G. Thiel, A. Moroni, and D. Parcej. 2007. Molecular properties of Kcv, a virus encoded K+ channel. *Biochemistry.* 46:1079–1090. http://dx.doi.org/10.1021/bi061530w

Plugge, B., S. Gazzarrini, M. Nelson, R. Cerana, J.L. Van Etten, C. Derst, D. DiFrancesco, A. Moroni, and G. Thiel. 2000. A potassium channel protein encoded by chlorella virus PBCV-1. *Science.* 287:1641–1644. http://dx.doi.org/10.1126/science.287.5458.1641

Santos, J.S., S.M. Grigoriev, and M. Montal. 2008. Molecular template for a voltage sensor in a novel K^+ channel. III. Functional reconstitution of a sensorless pore module from a prokaryotic Kv channel. *J. Gen. Physiol.* 132:651–666. http://dx.doi.org/10.1085/jgp.200810077

Tayefeh, S., T. Kloss, M. Kreim, M. Gebhardt, D. Baumeister, B. Hertel, C. Richter, H. Schwalbe, A. Moroni, G. Thiel, and S.M. Kast. 2009. Model development for the viral Kcv potassium channel. *Biophys. J.* 96:485–498. http://dx.doi.org/10.1016/j.bpj.2008.09.050

Villalba-Galea, C.A., W. Sandtner, D.M. Starace, and F. Bezanilla. 2008. S4-based voltage sensors have three major conformations. *Proc. Natl. Acad. Sci. USA.* 105:17600–17607. http://dx.doi.org/10.1073/pnas.0807387105